Synthesis and Solid State Chemistry of CH_3BiI_2: A Structure with an Extended One-Dimensional Organometallic Framework

Shumin Wang,[†] David B. Mitzi,*[,†] Gregory A. Landrum,[‡] Hugh Genin,[‡] and Roald Hoffmann[‡]

Contribution from the IBM T. J. Watson Research Center, P.O. Box 218, Yorktown Heights, New York 10598, and the Department of Chemistry and the Materials Science Center, Cornell University, Ithaca, New York 14853

Received May 23, 1996[⊗]

Abstract: Red needle-like crystals of the title compound were grown using a reaction between Bi metal and methyl iodide under solvothermal conditions. CH_3BiI_2 crystallizes in the monoclinic space group *C*2/*m* with an unusual one-dimensional organic−inorganic chain-like structure. The Bi atoms have a square pyramidal local geometry, with four I atoms forming the base and one methyl group occupying an apical site. Each basal square shares trans edges with two nearest neighbors to form a one-dimensional inorganic BiI_2 chain along the *b*-axis. All methyl groups are covalently bonded to bismuth atoms and are aligned on one side of the BiI_2 basal plane. The organic−inorganic chains are held together via van der Waals interaction, forming an extended solid state structural array. Extended Hückel band structure calculations demonstrate electronic one-dimensionality for CH_3BiI_2. Molecular modeling suggests that the square pyramidal Bi coordination arises primarily to reduce Bi−C antibonding character in the HOMO. The resulting Bi 6s and 6p hybridization in the valence band (HOMO) leads to a stereochemically active lone pair oriented trans to each methyl group. Thermal stability and decomposition of the title compound is examined using GC mass spectroscopy and simultaneous TGA and DTA techniques. CH_3BiI_2 begins to decompose at 185 °C in an inert atmosphere into methyl iodide and bismuth monoiodide, providing a new pathway to the formation of the interesting low valency one-dimensional conductor, BiI.

Introduction

Hybrid organic−inorganic compounds, which combine an extended inorganic framework with organic species, are involved in various fundamental as well as more applied studies related to their transport,[1−3] optical,[3−7] magnetic,[3,8,9] thermochromic,[10] or structural[7,11−14] properties. It is expected that these properties can be enhanced or fine tuned through the coupling between the organic and inorganic components of the structure. The integration of TiO_x and copper phthalocyanine (CuPc), for example, within an organic−inorganic heteromultilayer structure, leads to 40 times higher photoconductivity than in a CuPc single layer.[15] Ultimately, new physical properties, such as excitonic superconductivity,[16] may be envisioned if an appropriate coupling between organic and inorganic components can be achieved.

Generally speaking, there are three types of compounds in the category of extended organic−inorganic materials: (a) layered intercalated compounds, (b) ionic salts, and (c) covalently bonded compounds.[17] Type (a) compounds are created by intercalating organic species into the van der Waals gap between the inorganic layers. The inorganic and organic segments are often independently charge neutral, with the organic molecules acting as a guest species. The relevant bonding distances between the organic and inorganic components are fairly long, being governed by van der Waals interaction. This type of compound has been largely observed and studied in layered transition metal oxide, chalcogenide, and phosphate systems.[18−20]

For type (b) compounds, the organic component is an intimate part of the overall structure. A reasonable degree of coupling can be achieved through ionic and hydrogen bonding between the organic and inorganic parts of the structure, although the

* To whom correspondence should be addressed.
† IBM T. J. Watson Research Center.
‡ Cornell University.
⊗ Abstract published in *Advance ACS Abstracts,* January 1, 1997.

(1) Mitzi, D. B.; Feild, C. A.; Harrison, W. T. A.; Guloy, A. M. *Nature* **1994**, *369*, 467.
(2) Mitzi, D. B.; Wang, S.; Feild, C. A.; Chess, C. A.; Guloy, A. M. *Science* **1995**, *267*, 1473.
(3) Marsden, I. R.; Allan, M. L.; Friend, R. H.; Kurmoo, M.; Kanazawa, D.; Day, P.; Bravic, G.; Chasseau, D.; Ducasse, L.; Hayes, W. *Phys. Rev. B* **1994**, *50*, 2118.
(4) Ishihara, T.; Takahashi, J.; Goto, T. *Phys. Rev. B* **1990**, *42*, 11099.
(5) Calabrese, J.; Jones, N. L.; Harlow, R. L.; Thorn, D.; Wang, Y. *J. Am. Chem. Soc.* **1991**, *113*, 2328.
(6) Papavassiliou, G. C.; Koutselas, I. B.; Terzis, A.; Whangbo, M.-H. *Solid State Commun.* **1994**, *91*, 695.
(7) Mitzi, D. B. *Chem. Mater.* **1996**, *8*, 791.
(8) Willet, R. D.; Wong, R. J.; Numata, M. *Inorg. Chem.* **1983**, *22*, 3189.
(9) Rubenacker, G. V.; Haines, D. N.; Drumheller, J. E. *J. Magnet. Magnet. Mater.* **1984**, *43*, 238.
(10) Mostafa, M. F.; Abdel-Kader, M. M.; Arafat, S. S.; Kandeel, E. M. *Physica Scr.* **1991**, *43*, 627.
(11) Arend, H.; Tichy, K.; Baberschke, K.; Rys, F. *Solid State Commun.* **1976**, *18*, 999.
(12) Tieke, B.; Chapuis, G. *Mol. Cryst. Liq. Cryst.* **1986**, *137*, 101.
(13) Needham, G. F.; Willett, R. D.; Franzen, H. F. *J. Phys. Chem.* **1984**, *88*, 674.
(14) Wang, S.; Mitzi, D. B.; Field, C. A.; Guloy, A. M. *J. Am. Chem. Soc.* **1995**, *117*, 5297.
(15) Takada, J.; Awaji, H.; Koshioka, M.; Nakajima, A.; Nevin, W. A. *Appl. Phys. Lett.* **1992**, *61*, 2184.
(16) Little, W. A. *Phys. Rev. A* **1964**, *135*, 1416.
(17) Similar categorizations have been provided by others. For example, see: Day, P. In *Handbook of Conducting polymers*; Skotheim, T. A., Ed.; Marcel Dekker, Inc.: New York and Basel, 1986; Vol. 1, Chapter 4.
(18) Ogawa, M.; Kuroda, K. *Chem. Rev.* **1995**, *95*, 399, and references therein.
(19) (a) Jacobson, A. J. In *Solid State Chemistry: Compounds*; Cheetham, A. K., Day, P., Eds.; Oxford University Press: Oxford, 1992. (b) O'Hare, D. In *Inorganic Materials*; Bruce, D. W., O'Hare, D., Eds.; Wiley: Chichester, 1992. (c) Whittingham, M. S. *Prog. Solid State Chem.* **1978**, *12*, 41. (d) Whittingham, M. S.; Dines, M. B. *Surv. Prog. Chem.* **1980**, *9*, 55.
(20) (a) Clearfield, A. *Chem. Rev.* **1988**, *88*, 125. (b) Alberti, G.; Constantino, U. In *Intercalation Chemistry*; Whittingham, M. S., Jacobson, A. J., Eds.; Academic Press: New York, 1982; Chapter 5.

S0002-7863(96)01753-2 CCC: $14.00

electronic interaction is limited to some extent due to the ionic nature of the bonding. These compounds are mainly formed in transition and main group metal halides with layered or one-dimensional perovskite-related structures.[1,2,5−7,14,17] In the family $(C_mH_{2m+1}NH_3)_2(CH_3NH_3)_{n-1}Sn_nI_{3n+1}$, for example, conducting "*n*"-layer thick perovskite anion slabs alternate with much wider bandgap alkylammonium cation bilayers,[1] providing an interesting multilayer quantum well structure in which the well width can be controlled by *n* and the barrier layer thickness can be controlled through "*m*".

Compared to the first two classes, type (c) compounds are relatively unexplored. Although there are numerous reported compounds with covalent bonding between organic and inorganic components, most features isolated molecules or clusters. A few examples, however, including $Zr(HPO_4)(CH_{2n+1}PO_4)_yH_2O$,[21] $Zr(HPO_3)_{1.2}(O_3P\text{-}R\text{-}PO_3)_{0.4}$ (R = $Me_2H_2C_6C_6H_2Me_2$),[22] and CH_3ReO_3,[23] contain an extended inorganic framework. The former two compounds consist of Zr phosphate/phosphite layers with long-chain organic groups covalently bonded to them through P−O bonds. The latter one features two-dimensional ReO_3 layers. While the covalent bonding between the methyl group and the Re atom is well established in this compound, the structural details for the organic component is not yet completely determined. The strong covalent bonding in type (c) structures is expected to improve electronic communication between the organic and inorganic segments of the structure, creating the possibility of enhanced electronic tunability. Further investigation of covalently bonded organic−inorganic compounds, in particular among the organometallic halides, is the motivation of this work.

Among a number of known organometallic crystal structures, it has been observed that organo bismuth and antimony dihalide compounds have a strong tendency to form more than three intramolecular bonds and instead assume a distorted square pyramidal five-coordination around the Group 15 element,[24] with the organic group in an apical site and four halogens in the basal plane of the pyramid. For such compounds, without additional ligands, this often results in extended one-dimensional edge-sharing polymeric structures in which both halides are involved in bridging interactions, as found in $PhBiBr_2$,[25] $PhSbX_2$(X = Cl, Br, I),[26] $Sb(4\text{-}MeC_6H_4)X_2$ (X = Cl, Br),[27] and $MeSbX_2$ (X = Cl, Br, I).[28] CH_3SbI_2 is a particularly interesting example, yielding one of the simplest systems, with a unique one-dimensional organic−inorganic structure in which the methyl groups are ordered on one side of each SbI_2 chain. The extended chains in this compound, however, are disrupted by alternately short and very long pairs of Sb−I bonds, leading to a pseudo-trigonal pyramidal local geometry for Sb(III) and an alternate description of this compound in terms of weakly interacting CH_3SbI_2 molecular units.

In general, the more diffuse $n = 6$ lone pair electrons of Bi(III) might be expected to exhibit less stereochemical activity than those of Sb(III). The question of lone pair stereoactivity is, however, not trivial for bismuth compounds, as demonstrated in Bi_2WO_6. In this compound, the Bi(III) lone pairs play a crucial role in the structural chemistry, resulting in nominal BiO_4 pyramids in the Bi_2O_2 layers.[29] In contrast, for BiI_3 the solid state structure displays a symmetrical octahedral coordination of iodine ions about Bi(III), indicating a stereochemically "inert" lone pair.[30,31]

The Bi substituted analog of CH_3SbI_2 was first synthesized by Marquardt in 1887[32] by reacting $(CH_3)_3Bi$ with methyl iodide at 200 °C. Despite the usefulness of CH_3BiI_2 and related organobismuth dihalides in organometallic synthesis,[33] little has been reported on the solid state properties of these materials. In this report, we use a one step reaction between readily available methyl iodide and bismuth metal, under solvothermal conditions, to grow CH_3BiI_2 crystals with reasonable size, quality, and yield, without the need for preparing or handling the spontaneously combustible $(CH_3)_3Bi$ precursor. The single crystal structural study and extended Hückel calculations presented here elucidate the solid state chemistry of this interesting one-dimensional organometallic material. Of particular interest is the issue of the Bi(III) lone pair stereochemistry in CH_3BiI_2.

Experimental Section

Synthesis. Crystals of the title compound were grown from the reaction between Bi metal and CH_3I in an acid digestion bomb (23 mL, Parr 4749) under solvothermal conditions. An excess of methyl iodide was used as the solvent. Bi spheres (0.200 g) (−60 + 200 mesh, 99.999%, Aesar) were loaded into a quartz cup, which fit into the Teflon liner of the bomb. This was performed in a standard drybox with oxygen and water levels maintained below 1 ppm. Five milliliters of methyl iodide (99.5%, Aldrich) was then transferred into the quartz cup via a syringe under flowing nitrogen gas outside of the drybox. Different runs were carried out at various temperatures. The reaction occurred very slowly at 100 °C, while at 150 °C BiI_3 crystals started to form in addition to the title compound. The best temperature for the reaction was found to be around 125 °C. Most of the reactions were held at the desired temperature for 7 to 10 days, after which the furnace was turned off and allowed to cool naturally to room temperature. Prolonged reaction time generated a higher yield and larger crystals. For a reaction carried out at 125 °C for 10 days, the yield of CH_3BiI_2 was in excess of 40%, with numerous elongated crystals measuring up to 12 mm in length. A brick red powder, identified as BiOI by X-ray diffraction, was also obtained as a byproduct, suggesting some oxygen contamination during the process of closing the bomb or from the methyl iodide, which was used as received (i.e., undistilled). The red needle- or column-like crystals of the title compound, which readily frayed into thinner fibers, could be easily manually separated from any unreacted Bi spheres. A chemical analysis of the needles, performed by Galbraith Laboratories, was consistent with the formula CH_3BiI_2, despite problems with interference between Bi and I during the analysis (expected: C (2.51%), H (0.63%) I (53.12%), Bi (43.74%); found: C (2.49%), H (<0.5%), I (53.39%), Bi (42.13%)). The title compound appears to be relatively air stable. Powder X-ray diffraction yielded an identical pattern after the sample remained in air for 2 days. However, a few extra weak lines started showing in the powder pattern after 10 days exposure to air.

(21) Yamanaka, S.; Hattori, M. *Chem. Lett.* **1979**, 1073.
(22) Alberti, G.; Costantino, U.; Marmottini, F.; Vivani, R.; Zappelli, P. *Angew. Chem., Int. Ed. Engl.* **1993**, *32*, *No. 9*, 1357.
(23) (a) Herrmann, W. A.; Fischer, R. W. *J. Am. Chem. Soc.* **1995**, *117*, 3223. (b) Genin, H. S.; Lawler, K. A.; Hoffmann, R.; Herrmann, W. A.; Fisher, R. W.; Scherer, W. *J. Am. Chem. Soc.* **1995**, *117*, 3244.
(24) Carmalt, C. J.; Cowley, A. H.; Decken, A.; Norman, N. C. *J. Organomet. Chem.* **1995**, *496*, 59.
(25) Clegg, W.; Elsegood, M. R. J.; Errington, R. J.; Fisher, G. A.; Norman, N. C. *J. Mater. Chem.* **1994**, *4*, 891.
(26) Mundt, O.; Becker, G.; Stadelmann, H.; Thurn, H. *Z. Anorg. Allg. Chem.* **1992**, *617*, 59.
(27) Millington, P. L.; Sowerby, D. B. *J. Organomet. Chem.* **1994**, *480*, 227.
(28) (a) Breunig, H.-J.; Denker, M.; Ebert, K. H. *J. Organomet. Chem.* **1994**, *470*, 87. (b) Breunig, H.-J.; Ebert, K. H.; Gülec, S.; Dräger, M.; Sowerby, D. B.; Begley, M. J.; Behrens, U. *J. Organomet. Chem.* **1992**, *427*, 39.
(29) Watanabe, A. *Mat. Res. Bull.* **1984**, *19*, 877.
(30) Galy, J.; Enjalbert, R. *J. Solid State Chem.* **1982**, *44*, 1.
(31) Schlueter, M.; Cohen, M. L.; Kohn, S. E.; Fong, C. Y. *Phys. Stat. Sol. B* **1976**, *78*, 737.
(32) Marquardt, A. *Chem. Ber.* **1887**, *20*, 1516.
(33) Freedman, L. D.; Doak, G. O. *Chem. Rev.* **1982**, *82*, 15, and references therein.

X-ray Crystallography. Suitable single crystals were selected under a microscope (inside the drybox) and sealed in quartz capillaries. A thin needle-like crystal (0.01 mm × 0.04 mm × 0.5 mm) was chosen for the structural study. Data for the title compound were collected at room temperature on an Enraf-Nonius CAD4 diffractometer with graphite monochromatized Mo Kα radiation. The data collection parameters and the structural refinement results are presented in Table 1. Unit cell parameters and the crystal orientation matrix were obtained by least-squares fit of 25 reflections with $18° < 2\theta < 40°$. Three intensity control reflections were monitored every 5000 s during the data collection. No sign of X-ray induced degradation of the crystal was noted during the data collection process. The NRCVAX 386 PC version[34] program was used for the structural solution and refinement. The intensity data were corrected for Lorentz and polarization effects, and the refinement was performed using the counting statistics weighting scheme. Empirical absorption corrections based on several azimuthal scans were also applied, yielding transmission factors ranging from 0.179 to 0.438.

Three possibilities for choosing the space group—*C*2/*m*, *Cm*, and *C*2—were consistent with the observed systematic conditions: *hkl*, $h + k = 2n$; *h*0*l*, $h = 2n$; 0*kl*, $k = 2n$; *hk*0, $h + k = 2n$; 0*k*0, $k = 2n$; *h*00, $h = 2n$. The centrosymmetric space group, C2/m, was finally chosen over the noncentrosymmetric space groups, *C*2 and *Cm*, because an inversion center was detected, using the program MISSYM,[35] for the arrangements of atoms found in the noncentrosymmetric space groups. In addition, refinement in the space group *C*2 did not lower the *R* values despite more refined parameters (the final refinements yielded the following results for the R/R_w factors and goodness of fit (GoF): 0.038/0.048; 1.60 and 0.048/0.064; 2.05 for the space groups *C*2/*m* and *C*2, respectively). The refinement in the *Cm* space group was highly unstable (i.e., never converged). Furthermore, there were no anomalous thermal parameters for the refinement in the centrosymmetric space group.

The positions of the heavy atoms, Bi and I, were determined by direct methods, while the atomic positions for carbon were picked up from the Fourier difference maps. Locating the hydrogen atoms was not attempted. Anomalous dispersion effects were included during the refinement. The bismuth and iodine atomic displacement parameters were refined anisotropically, while those of the light carbon atoms were refined isotropically. The atomic positions and isotropic thermal parameters of the title compound are presented in Table 2, while the anisotropic temperature factors for the heavy atoms are supplied as Supporting Information (Table S.1). The minimum and maximum peaks in the final difference Fourier map corresponded to −2.28 and 2.39 e/Å^3, with the largest residual peak appearing approximately 0.77 Å away from the Bi(1) atom.

Thermal Stability Studies. The thermal behavior of the title compound was studied by both conventional thermal analysis and gas chromatography/mass spectroscopy (GC/MS). Simultaneous thermogravimetric (TGA) and differential thermal analysis (DTA) were performed on the title compound, using a Setaram TAG 24 thermal analysis system. Each run was performed on approximately 40−60 mg of sample at a ramp rate of 1 °C/min in an argon atmosphere. Tantalum crucibles were used for containers. Special care was taken to exclude oxygen from the apparatus by evacuating and backfilling the thermal analysis apparatus with argon several times. The temperature was calibrated using the melting transitions of indium (T_m = 156.6 °C), tin (T_m = 231.9 °C), and bismuth (T_m = 271.3 °C), using the same system configuration (crucible type, temperature ramp rate, gas type, gas flow, etc.). Several thermal analysis scans were performed to evaluate each decomposition step for CH_3BiI_2. Each scan was terminated immediately above the relevant decomposition step, and the products were identified by X-ray powder diffraction using a Siemens D5000 diffractometer, after cooling to room temperature.

GC/MS was performed using a SIS (Scientific Instrument Services) thermal desorption unit and a Hewlett Packard 5988A mass spectrometer. The interface between the instruments was a gas chromatograph fitted with a 30 cm unlined capillary silica tube in place of a standard GC column. The GC column was held at 325 °C to assure transfer of all volatile species formed. The sample (0.8 mg) was loaded into the thermal desorption unit and heated at a rate of 2 °C/min in helium. Mass spectra were recorded throughout the heating cycle (30 °C to 450 °C).

(34) Gabe, E. J.; Le Page, Y.; Charland, J.-P.; Lee, F. L.; White, P. S. *J. Appl. Crystallogr.* **1989**, *22*, 384.

Table 1. Parameters of Data Collection and Structure Refinement for CH_3BiI_2

formula	CH_3BiI_2
formula weight	477.82
crystal color	dark red
crystal system	monoclinic
space group	*C*2/*m*
a, Å	15.611(1)
b, Å	4.3485(4)
c, Å	19.297(2)
β, deg	106.395(6)
V, Å^3	1256.6(2)
Z	8
ρ_{calcd}, g/cm^3	5.051
radiation (λ), Å	Mo Kα (0.7107)
absorption coeff (μ), cm^{-1}	375.7
scan mode	$\omega-2\theta$
2θ range, deg	$3.0 \le 2\theta \le 55.0$
data collected	$h,\pm k,\pm l$
R_{int}	0.095
no. of data collected	3057
no. of unique data	1643
no. of data used in refinement	1201 ($I > 3\sigma(I)$)
no. of variables	44
secondary extinction coefficient (μm)	0.473
R_F[a]	0.038
R_w[b]	0.048
goodness of fit (GoF)[c]	1.60

[a] $R_F = \sum(F_o - F_c)/\sum(F_o)$. [b] $R_w = \{\sum w(F_o - F_c)^2/\sum(wF_o^2)\}^{1/2}$. [c] GoF $= \{\sum w(F_o - F_c)^2/(n - m)\}^{1/2}$; n = number of reflections, m = number of refinement parameters.

Table 2. Positional and Isotropic Thermal Parameters[a] for CH_3BiI_2

atom	*x*	*y*	*z*	B_{iso} (Å^2)
Bi(1)	0.82798(4)	0.0	0.34450(3)	2.72(3)
Bi(2)	0.93846(4)	0.0	0.15635(3)	2.73(3)
I(1)	0.97622(7)	0.5	0.35985(6)	3.19(5)
I(2)	0.68635(7)	0.5	0.34070(6)	3.01(5)
I(3)	0.79455(7)	0.5	0.15523(6)	2.88(5)
I(4)	0.07346(7)	0.5	0.14351(6)	3.20(5)
C(1)	0.859(1)	0.0	0.468(1)	3.8(3)
C(2)	0.884(1)	0.0	0.035(1)	3.9(3)

[a] Heavy atoms (Bi and I) are refined anisotropically.

Table 3. Selected Bond Distances (Å) and Angles (deg) in CH_3BiI_2

Bi(1)−I(1)	3.128(1)	Bi(2)−I(3)	3.122(1)
Bi(1)−I(1)[a]	3.128(1)	Bi(2)−I(3)[a]	3.122(1)
Bi(1)−I(2)	3.087(1)	Bi(2)−I(4)[b]	3.086(1)
Bi(1)−I(2)[a]	3.087(1)	Bi(2)−I(4)[c]	3.086(1)
Bi(1)−C(1)	2.29(2)	Bi(2)−C(2)	2.26(2)
I(1)−Bi(1)−I(1)[a]	88.08(3)	I(3)−Bi(2)−I(3)[a]	88.28(3)
I(1)−Bi(1)−I(2)	91.06(2)	I(3)−Bi(2)−I(4)[b]	90.87(2)
I(1)−Bi(1)−I(2)[a]	176.06(4)	I(3)−Bi(2)−I(4)[c]	175.13(4)
I(1)[a]−Bi(1)−I(2)	176.06(4)	I(3)[a]−Bi(2)−I(4)[b]	175.13(4)
I(1)[a]−Bi(1)−I(2)[a]	91.06(2)	I(3)[a]−Bi(2)−I(4)[c]	90.87(2)
I(2)−Bi(1)−I(2)[a]	89.55(3)	I(4)[b]−Bi(2)−I(4)[c]	89.58(3)
I(1)−Bi(1)−C(1)	88.2(3)	I(3)−Bi(2)−C(2)	86.2(3)
I(1)[a]−Bi(1)−C(1)	88.2(3)	I(3)[a]−Bi(2)−C(2)	86.2(3)
I(2)−Bi(1)−C(1)	87.9(3)	I(4)[b]−Bi(2)−C(2)	89.0(3)
I(2)[a]−Bi(1)−C(1)	87.9(3)	I(4)[c]−Bi(2)−C(2)	89.0(3)

[a] $x, -1 + y, z$. [b] $1 + x, y, z$. [c] $1 + x, -1 + y, z$.

Results and Discussions

Structural Description. The title compound crystallizes in the monoclinic space group, C2/m. Single crystal structural studies yielded the composition CH_3BiI_2, in agreement with the

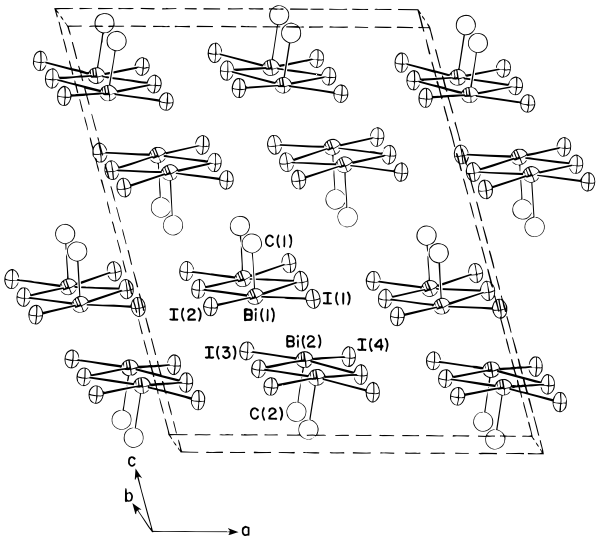

Figure 1. An ORTEP drawing of the unit cell of CH_3BiI_2, viewed approximately along the *b*-axis, with the unit cell outlined. All the atoms are drawn at 50% probability. The ellipsoids for bismuth and iodine atoms represent their anisotropic thermal parameters. The carbon atoms (refined isotropically) are drawn as open circles.

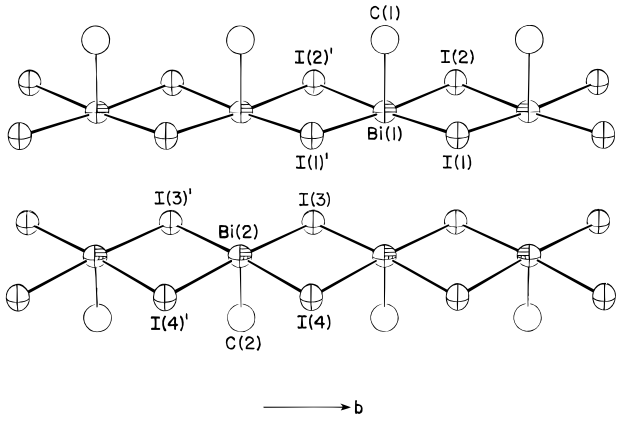

Figure 2. The one-dimensional CH_3BiI_2 chains extending along the *b*-axis.

chemical analysis results ($C_{1.0(2)}Bi_{1.0(2)}I_{2.1(1)}$). Figure 1 shows the ORTEP drawing of a unit cell of CH_3BiI_2, viewed along the *b*-axis. In this structure, there are two independent bismuth sites in an asymmetric unit, each with a square pyramidal coordination. The Bi atoms connect to four iodines, with the bond lengths, 3.087(1) Å (2×) and 3.128(1) Å (2×) for Bi(1), and 3.086(1) Å (2×) and 3.122(1) Å (2×) for Bi(2), forming a slightly distorted basal square coordination. The pyramid is completed by a fifth coordination of Bi to a methyl group in the apical site. Each basal square shares trans edges with two nearest neighbors, forming a one-dimensional inorganic BiI_2 chain along the *b*-axis, with a 4.3485(4) Å Bi−Bi distance along the chain. The methyl groups are aligned on one side of each BiI_2 chain, as shown in Figure 2. The two independent bismuth sites correspond to two symmetry-inequivalent CH_3BiI_2 chains which, however, are very similar in geometry. The one-dimensional chains are weakly held together by van der Waals interaction forming the extended solid state structure.

A similar local environment for bismuth, square pyramidal five coordination, was also recently found in several other organobismuth halides, such as $PhBiBr_2$,[25] $[NEt_4]_2[Bi_2Ph_2I_6]\cdot Et_2O$,[36] and $[NBu^n_4]_2[Bi_2Ph_2Br_6]$.[37] However, $PhBiBr_2$ forms an edge shared zigzag chain-like structure, with phenyl groups alternately located on the two sides of the chain. The latter two compounds contain isolated bismuth dimeric complexes. The observed Bi−C bond distances (2.29(2) Å for Bi(1)−C(1) and 2.26(2) Å for Bi(2)−C(2)) in CH_3BiI_2 are comparable to the reported values in the above mentioned examples.

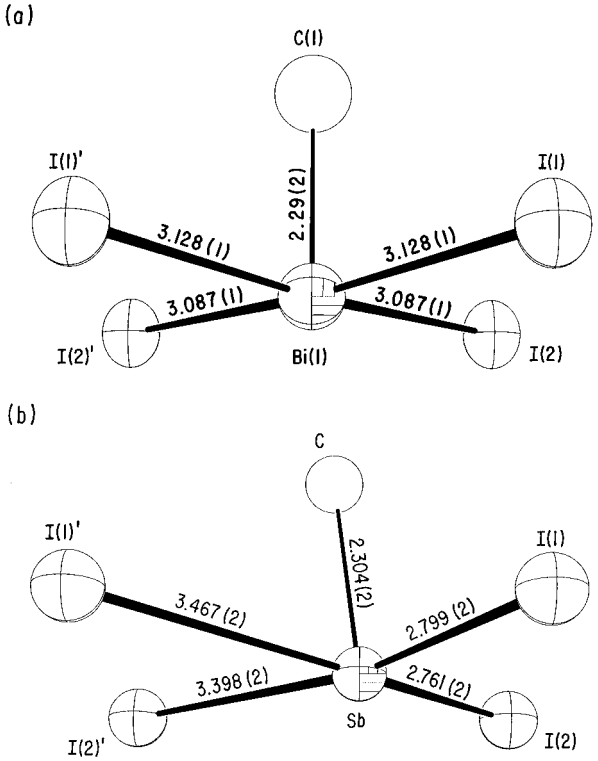

Figure 3. ORTEP drawings of the five-coordinated local environments in CH_3MI_2, for M = Bi (a), and M = Sb (b), highlighting the difference in the degree of distortion for the two Group 15 metal atoms.

In CH_3BiI_2 and the above mentioned compounds, bismuth has a +3 formal oxidation state. In principle, this leaves a pair of nonbonding electrons which have the potential to be stereochemically active. Structurally, the square pyramidal geometry for bismuth provides an open coordination site (trans to the methyl group) which is likely to be filled by these lone pair electrons. The fact that the Bi lies approximately 0.11 Å below the plane of the iodines also fits well with the idea of there being a stereochemically "active" lone pair—from a valence shell electron pair repulsion (VSEPR) argument,[38] the iodines can be viewed as being bent away from the lone pair site by lone pair-bonding pair repulsion.

Structural Comparison to CH_3SbI_2 and Lone Pair Stereochemical Activity of the Group 15 Elements. The structure of CH_3BiI_2 is related to that of the distinct compound, CH_3SbI_2[28] in that they both nominally have inorganic one-dimensional $(Bi,Sb)I_2$ chains, with methyl groups covalently bonded to the Bi/Sb atoms on one side of the $(Bi, Sb)I_2$ basal plane. However, CH_3SbI_2 crystallizes in the triclinic space group $P\bar{1}$, with the Sb(III) coordination sphere significantly distorting away from the square pyramidal Bi(III) coordination of CH_3BiI_2. Sb(III) principally bonds to two iodines (2.799 Å and 2.761 Å) and one carbon (2.30 Å) (Figure 3). The full coordination is completed by two much more distant iodines

(35) Le Page, Y. *J. Appl. Crystallogr.* **1988**, *21*, 983.

(36) Clegg, W.; Errington, R. J.; Fisher, G. A.; Hockless, D. C. R.; Norman, N. C.; Orpen, A. G.; Stratford, S. E. *J. Chem. Soc., Dalton Trans.* **1992**, 1967.

(37) Clegg, W.; Errington, R. J.; Fisher, G. A.; Flynn, R. J.; Norman, N. C. *J. Chem. Soc., Dalton Trans.* **1993**, 637.

(38) Gillespie, R. J.; Nyholm, R. S. *Quart. Rev. Chem. Soc.* **1957**, *11*, 339.

(3.467 Å and 3.398 Å), which extend the CH_3SbI_2 molecular unit into a pseudo-chain. These latter two iodines are sufficiently distant from Sb(III) (on average, over 20% farther than the two close iodines) that the antimony structure can perhaps most appropriately be considered as an intermediate between a molecular structure with trigonal pyramidal Sb(III) coordination and an extended structure with a highly-distorted square pyramidal coordination. This is in contrast to CH_3BiI_2, which clearly adopts an extended solid state structure, with intrachain Bi−I bond lengths in the relatively narrow range, 3.086−3.128 Å. The dark red coloration of CH_3BiI_2 may partially arise from greater orbital overlap along the chain relative to the yellow CH_3SbI_2.

One can try to understand the local geometries of bismuth and antimony in the present compounds by classical electrostatics and a simple consideration of the Bi(III) and Sb(III) lone pair stereoactivity. The general concept of lone pair stereochemistry is widely discussed in the literature and is typically structurally-based, most often invoked for molecular or solid state structures containing elements with one formal nonbonding electron pair. When one finds a coordination geometry that is less than maximally symmetrical, and the geometry leaves some space for what appears to be a lone pair, this electron pair, or more loosely the compound containing it, is described as being stereochemically active. Early work in the area of lone pair stereochemistry includes a general consideration of stereochemical types and valency groups by Sidgwick and Powell[39] in 1940. According to this work, the arrangements in space of the covalencies of multicovalent atoms are very simply related to the size of the valency shell of electrons. The pairs of electrons in a valency shell are generally arranged in the same way depending only on their numbers, irrespective of whether they are shared (i.e., bonding) pairs or unshared (i.e., nonbonding) pairs. Thus, two pairs are arranged linearly, three pairs in a plane triangle, four pairs in a tetrahedron, five pairs in a trigonal bipyramid, and six pairs in an octahedron. Gillespie and Nyholm[38] have extended this idea considerably in their VSEPR model. If some of the electrons are lone pairs, or if there are two or more different kinds of attached atom or group, deviations from the regular structures are to be expected. In the CH_3BiI_2 structure, bismuth atoms have six pairs of electrons in their valency shell: four pairs bonded to iodine atoms, one pair bonded to a methyl group, and one nonbonded (lone) pair. An "octahedral" coordination is expected. Therefore from the structural point of view it is natural to assume that the lone pair electrons are stereochemically "active" and are located in the open site trans to the methyl group, completing the (pseudo) octahedral coordination for the bismuth atoms.

In general, the stereochemical activity of the lone pair appears to be more important for smaller more electronegative cations than for bigger ones—i.e., it increases going up a column from the bottom of the periodic table. In BiI_3, for example, Bi(III) adopts a regular octahedral coordination of iodine ligands (inert or "inactive" lone pair), whereas in SbI_3 and AsI_3 the octahedra trigonally distort to yield approximately C_{3v} symmetry, with three long and three short metal−halogen bond distances.[40] A similar situation occurs in the family CH_3MI_2 (M = Sb, Bi), although in this case the lone pairs play an active role in both structures. For CH_3BiI_2, the coordination is essentially octahedral, with the lone pair occupying the sixth ligand site. In CH_3SbI_2, the situation is more complicated. The local geometry for Sb(III) appears roughly square-pyramidal, but two Sb−I bonds are considerably weakened, leading to a significant distortion from the geometry observed in CH_3BiI_2. The lone pair appears to be "pointing" somewhere between the "empty" sixth coordination site and the two further iodine atoms.

While the VSEPR model has had great success explaining the geometries of molecules consisting of main group elements, it cannot account for why some compounds have a stereochemically inert lone pair, while others have an active lone pair. The detailed behaviors, such as the involvement in bonding and the evolution of the degree of stereochemical activities of lone pairs, can be better understood by molecular orbital studies. Recently, Wheeler and Kumar have applied extended Hückel molecular orbital and crystal orbital calculations to binary Group 15 halides.[40] While in this section we discussed lone pair stereoactivity using the somewhat loosely defined structurally-based language, a more detailed understanding, based on extended Hückel molecular modeling studies, is provided for the compound CH_3BiI_2 in the next section.

Electronic Structure Calculations for CH_3BiI_2. To probe the potential role played by lone pair formation in determining the structure of CH_3BiI_2, a molecular model of the bismuth coordination environment was constructed and studied using the extended Hückel method.[41] This model consists of a central Bi atom surrounded by four iodines and a single methyl group. To maintain the same oxidation states as found in the bulk structure, the molecule was given a charge of 2−, yielding the formula $(CH_3BiI_4)^{2-}$. The effect of lone pair formation at the bismuth atom was studied by distorting the coordination environment about the Bi from a trigonal bipyramid ("D_{3h}"), the most symmetrical arrangement of the five anions, to a square pyramidal ("C_{4v}") geometry. This was done by continuously varying the two 120° C−Bi−I bond angles (θ) in the trigonal bipyramidal geometry from 120° to 90°. The Bi−C bond length was set at the experimental value of 2.29 Å, with the CH_3 group being placed in the equatorial plane of the D_{3h} structure, while the Bi−I bond lengths were set to the average observed length, 3.1 Å.

As seen in the Walsh diagram in Figure 4, the system is stabilized by a distortion away from D_{3h} toward C_{4v} geometry. This stabilization arises from the substantial decrease in energy of the HOMO (the other occupied orbitals do not change significantly in energy with the distortion). In addition, the Lowest Unoccupied Molecular Orbital (LUMO) is destabilized as the system progresses toward the square pyramidal geometry.

The formation of the lone pair type orbital on Bi (the HOMO) as the distortion toward C_{4v} progresses can be monitored by following the percent contributions of the Bi 6s and $6p_x$ orbitals to the HOMO (the p_x orbital is involved in lone pair formation because the CH_3 group lies along the *x*-axis). Figure 5 demonstrates that the amount of Bi $6p_x$ that is mixed into the HOMO increases as we move toward the C_{4v} geometry—this is lone pair formation at the Bi atom. The polarization of the orbitals on the Bi (arising due to the s-p_x mixing) toward the empty space between the equatorial iodine atoms is visible in the contour plot of Figure 6 for the square pyramidal C_{4v} geometry. This is to be contrasted with the HOMO of the D_{3h} geometry. Here there is some s-p_x mixing (to reduce the amount of C−Bi antibonding character), but the geometry and the fact

(39) Sidgwick, N. V.; Powell, H. M. *Proc. R. Soc. London* **1940**, *176A*, 153.

(40) Wheeler, R. A.; Pavan Kumar, P. N. V. *J. Am. Chem. Soc.* **1992**, *114*, 4776.

(41) (a) Hoffmann, R. *J. Chem. Phys.* **1963**, *39*, 1392. (b) Parameters H_{ii}(eV) and STO exponent used in the EH band structure calculations: H 1*s*: −13.6, 1.3; C 2*s*: −21.4, 1.625; C 2*p*: −11.4, 1.625; I 5*s*: −18.0, 2.679; I 5*p*: −12.7, 2.322; Bi 6*s*: −15.19, 2.56; Bi 6*p*: −7.79, 2.072. All calculations were carried out using the program YAeHMOP, written by one of the authors (G. L.). YAeHMOP is freely available on the World Wide Web at URL http://overlap.chem.cornell.edu:8080/yaehmop.htm1

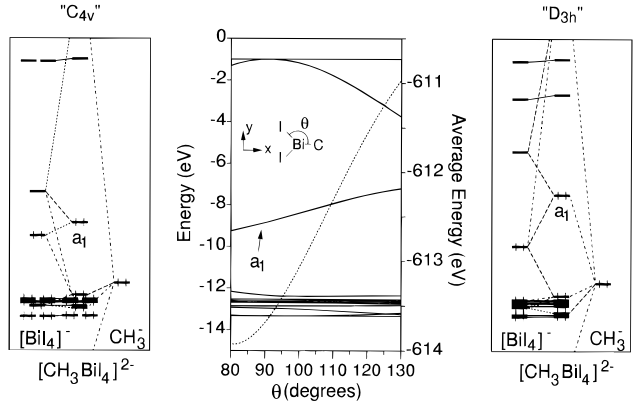

Figure 4. *Central panel:* A Walsh diagram for the distortion of $(CH_3BiI_4)^{2-}$ from the C_{4v} to the D_{3h} symmetry. Solid lines show the evolution of the MOs of the molecular model. The dashed line indicates the calculated total (average) energy values along the distortion. *Left and Right panels:* Fragment Molecular Orbital (FMO) interaction diagrams for the interaction of $(BiI_4)^-$ with $(CH_3)^-$ for the two geometries. The level marked a_1 is the Highest Occupied Molecular Orbital (HOMO) of the system.

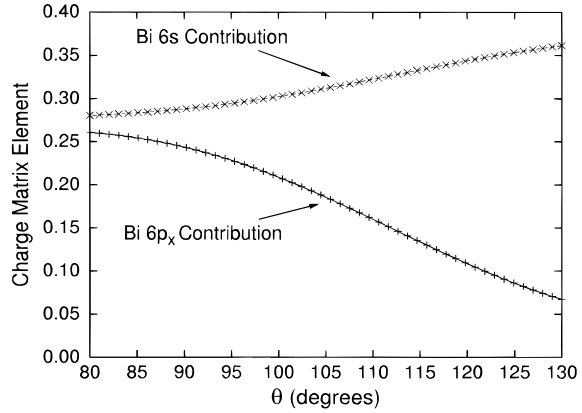

Figure 5. Fractional contributions (charge matrix elements) for Bi 6s and $6p_x$ to the HOMO of $(CH_3BiI_4)^{2-}$ as a function of the C−Bi−I bond angle, θ.

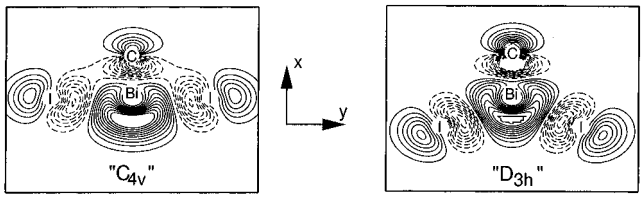

Figure 6. Contour plots (in the XY plane) of the HOMO for the $(CH_3BiI_4)^{2-}$ system in the C_{4v} and D_{3h} geometries. Positive phases are drawn with solid lines, negative phases with dashed lines. The contours start at $|\psi| = 0.01$ and progress in increments of ± 0.01.

that the orbital is antibonding between the Bi and the equatorial iodines prevents formation of a true lone pair type orbital on the Bi.

We can explore the driving force for the lone pair formation at the Bi atom by examining the Bi−C bonding character of the molecular orbitals in $(CH_3BiI_4)^{2-}$. The Molecular Orbital Overlap Population (MOOP) plots for the Bi−C bonds (Figure 7) show the contributions of individual molecular orbitals to a Mulliken overlap population. In the D_{3h} geometry, the HOMO (around −8 eV) is strongly Bi−C antibonding, while in the C_{4v} configuration, the HOMO is basically nonbonding between the Bi and C. The consequence of this lessening of Bi−C antibonding character in the HOMO is an increase in the Bi−C overlap population. The average Bi−C Mulliken overlap

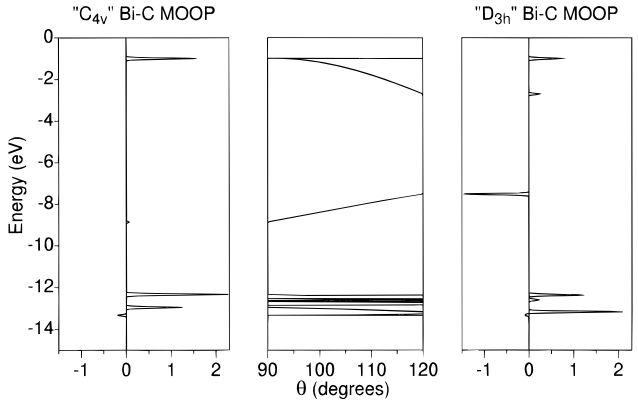

Figure 7. Bi−C Molecular Orbital Overlap Population (MOOP plots for $(CH_3BiI_4)^{2-}$ in the C_{4v} (left panel) and D_{3h} (right panel) geometries. The central panel has part of the Walsh diagram from Figure 4.

population reaches 0.508 for the square pyramidal (C_{4v}) geometry, while it is 0.405 for the trigonal bipyramidal (D_{3h}) geometry. In summary, the molecular model demonstrates that the reduction in the amount of Bi−C antibonding character drives the distortion of $(CH_3BiI_4)^{2-}$ from a D_{3h} to a C_{4v} geometry and the formation of the lone pair type orbital at the Bi site. This effect is probably also present in the solid state, accounting for the quasi-square pyramidal environments of the Bi atoms in CH_3BiI_2.

Certainly the most significant interactions within the CH_3BiI_2 structure occur within the chains. Thus we next consider a model in which a single CH_3BiI_2 chain is cut out of the full three-dimensional structure and examine its electronic structure. Specifically, the chain contains square pyramidal coordinated Bi(III) with Bi−C bonds of 2.29 Å, Bi−I bonds of 3.13 and 3.09 Å, and C−Bi−I bond angles of 88°, as observed in the real crystal. Hydrogen atoms were placed at idealized positions, with C−H bond lengths set at 1.09 Å.

An aufbau approach was used in order to understand the electronic structure of this chain by splitting it (theoretically) into two sublattices made of (1) a chain of CH_3Bi fragments and (2) a double chain of iodine ions. In a single CH_3Bi fragment, with the Bi−CH_3 bond lying along the *x*-axis (with the methyl group at more positive *x*), the CH_3 sp^3 hybrid orbital interacts with the 6s and $6p_x$ orbitals on the Bi to form the HOMO of the fragment. This orbital consists mainly of Bi 6s (18.5%), Bi $6p_x$ (33.8%), hybridized away from the carbon, and the sp^3 hybrid from the methyl group (44.3%). The LUMO is doubly degenerate and consists of almost pure $6p_y$ and $6p_z$ orbitals of Bi (99.2% each).

Next, a 1-D chain of these CH_3Bi fragments, at a distance of 4.35 Å running along the *z*-axis, was created. At this distance, the p−p σ-type overlap between Bi atoms is −0.11, which is not negligible, but also not large. We expect then that the orbitals of this chain will closely resemble those of the fragment; the band structure is shown in the left panel of Figure 8. The energies of the band midpoints are very close to those of the CH_3Bi fragment, which, along with the flatness, emphasizes how little interaction there is between CH_3Bi units.

In the right hand panel of Figure 8, we see the band structure for the iodine sublattice. Given the interiodine separation of approximately 4.4 Å, we expect very little interaction between them, as confirmed by the very flat nature of the I 5s and 5p bands. These bands are centered around the iodine H_{ii}'s of −18.0 and −12.7 eV for the 5s and 5p orbitals, respectively. When the interaction between the iodine and CH_3Bi sublattices is turned on (center panel of Figure 8), the largest changes are

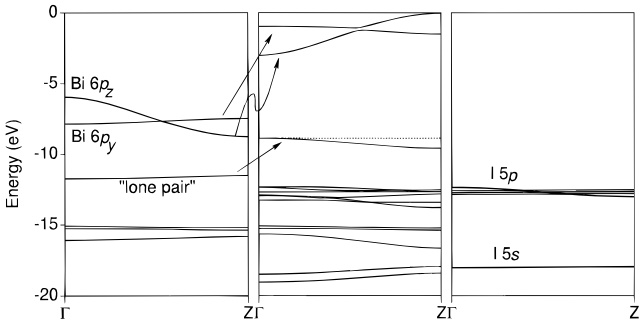

Figure 8. Band structure for a chain of CH_3Bi fragments (left panel), for a double chain of iodines (right panel), and for the 1-D CH_3BiI_2 chain (center panel), which is created by allowing the two fragmentary units to interact. The dotted line in the center panel indicates the position of the Fermi energy for the chain.

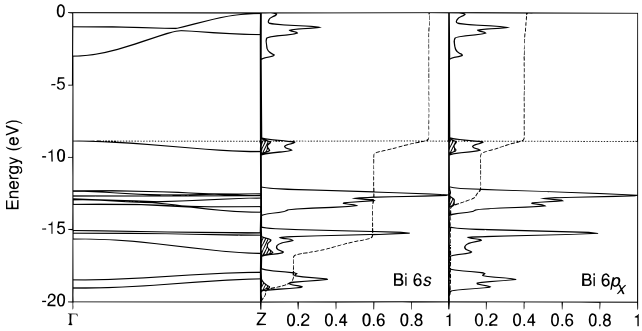

Figure 9. Band structure for the one-dimensional CH_3BiI_2 chain model (left panel) and projected density-of-states (DOS) curves for bismuth 6s (center panel) and $6p_x$ (right panel). Solid lines in the DOS plots give the total DOS, while hatched regions correspond to the projections; the dashed lines running up are the integrations of the projected states.

due to the Bi 6p orbitals being pushed up in energy by the iodine orbitals. These are the interactions involving the largest overlap.

The highest occupied band is transformed somewhat by interactions with the iodines, although it retains its character as a Bi "lone pair" band. The contribution from the methyl group has all but disappeared and is replaced by antibonding contributions from iodine. The lone pair band is fairly flat, but changes on going from the CH_3Bi chain to the full 1-D chain so that it runs "down" instead of "up" from Γ to Z as a result of interactions with I 5s and additionally $5p_x$ orbitals. Figure 9 displays the projected density-of-states (DOS) curves for the bismuth 6s and $6p_x$ contributions to the lone pair band. The highest occupied band consists of 28.9% Bi 6s, 24.2% Bi $6p_x$, 11.3% I(1), $5p_z$, 11.4% I(2) $5p_z$, 7.8% I(1) $5p_y$, and 7.9% I(2) $5p_y$, along with small contributions from I 5s, C 2s, and $2p_x$ orbitals. Likewise the lowest two unfilled bands consist primarily of Bi $6p_y$ and Bi $6p_z$ character.

For this single chain model, the Bi−C bond (2.29 Å) has an overlap population of 0.531, which is quite close to the value found in the molecular model for $(CH_3BiI_4)^{2-}$ in the C_{4v} geometry. The Bi−I overlap populations for the 3.09 and 3.13 Å bonds are 0.179 and 0.154, respectively. These two overlap populations are again fairly close to the value in the C_{4v} molecular model (0.157). The Crystal Orbital Overlap Population (COOP) curves for the Bi−C and Bi−I bonds (Figure 10) demonstrate that the highest occupied band is basically nonbonding between bismuth and carbon (with only 3.6% carbon), closely resembling the Bi−C MOOP in the molecular model, and strongly Bi−I antibonding.

To sum up, for the one-dimensional model of CH_3BiI_2, the band structure shows the chains to be insulating with a direct band gap of approximately 5.8 eV. The highest filled band

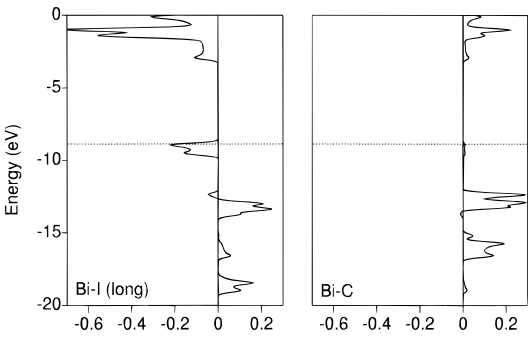

Figure 10. Crystal orbital overlap population (COOP) curves, for the Bi−C (right panel) and the longer of the two Bi−I (left panel) bonds, for the one-dimensional CH_3BiI_2 chain model.

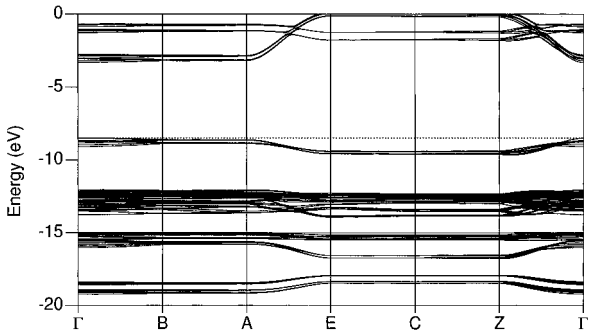

Figure 11. Band structure of the full 3-D CH_3BiI_2 structure. The positions of the special points in the first Brillouin zone are (in fractional coordinates): Γ (0 0 0), B (0.5 0 0), A (0.5 0 0.5), E (0.5, 0.5, 0.5), C (0 0.5 0.5), and Z (0 0.5 0). The dotted line indicates the position of the Fermi energy.

(valence band) is a lone-pair combination on bismuth, pointing away from the methyl group, which is pushed up in energy by interaction with mainly iodine 5p orbitals—it remains flat across the Brillouin zone as a result of the fairly long Bi−Bi distance. The lowest unoccupied bands are mostly bismuth $6p_z$ and $6p_y$, pushed up in energy by interaction with (again) mainly iodine 5p orbitals.

Because the one-dimensional chains are insulating, and the interaction between chains is probably weak, we expect the bands around the Fermi level to broaden just slightly in going to the full three-dimensional crystal structure calculation (Figure 11). This will cause a net destabilization due to what is essentially the same phenomenon as two-orbital-four-electron interactions, otherwise known as steric repulsion. Unsurprisingly, the calculated Fermi level in the bulk is raised (−8.42 eV versus −8.80 eV) and the calculated band gap is smaller (5.3 eV versus 5.8 eV) in the bulk than in the isolated chain. Note that extended Hückel calculations usually result in calculated band gaps which are too large. In fact, if one assumes that the compound absorbs at roughly 550 nm to appear red, the true band gap should be in the vicinity of 2−3 eV.

The directions A → E and Z → Γ correspond to the **b** axis of the real-space unit cell; this is the direction of propagation of the 1-D chains and thus it shows the most band dispersion and resemblance to the band structure of the 1-D model presented above. The exceedingly similar band structure of the full 3-D structure and the 1-D model highlights the small degree of coupling between the chains in the CH_3BiI_2 structure. The directions Γ → B and B → A correspond to the real space **a** and **c** axes, and show very little bandwidth, again demonstrating the electronic one-dimensionality of the title compound.

The interchain interactions are small but not entirely negligible. While the overlap population between Bi atoms on

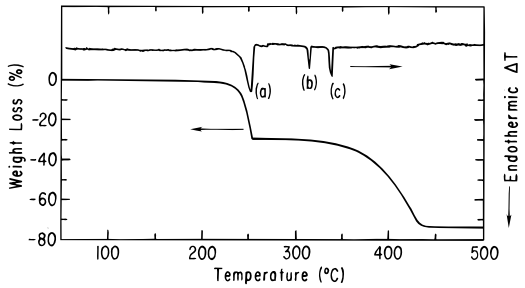

Figure 12. Simultaneous thermogravimetric analysis and differential thermal analysis scan for CH_3BiI_2, performed in flowing argon with a ramp rate of 1°/min. For clarity, only the heating portion of the curve is shown.

different chains is a tiny −0.003, the COOP curve reveals that there is some interaction. The value of the overlap population is low because the bonding and antibonding interactions between these two atoms almost exactly cancel in magnitude. Likewise, the Bi−I overlap populations range from −0.004 to −0.002. But here the COOP curves prove that there is truly very little interchain Bi−I interaction occurring. Another measure of the interaction is the energy spread of the lone-pair derived bands at Γ. If there were no interchain interaction, these eight bands would be degenerate (have no energy spread) at Γ. In the 3-D system, however, the spread in energies of the eight lone-pair bands is 0.56 eV, indicating that, while very small, there is some "cross-talk" between the chains.

Thermal Stability Studies. The thermal behavior of the organic-inorganic compound, CH_3BiI_2, was studied by both gas chromatography/mass spectroscopy and conventional thermal analysis. The GC/MS study demonstrates that the title compound is thermally stable in an inert (helium) atmosphere up to 185 °C, and then starts liberating methyl iodide. The process basically ends at 270 °C, although a small amount of methyl iodide was detected up to 285 °C. In vacuum, the title compound appears to slowly volatilize above approximately 130 °C, with some degree of decomposition observed as well. We have, however, grown single crystals by subliming CH_3BiI_2 in an evacuated quartz ampule in this temperature range.

Simultaneous thermogravimetric analysis (TGA) and differential thermal analysis (DTA) were carried out up to 500 °C in argon. The result is shown in Figure 12, demonstrating two weight loss processes (from TGA) and three endothermic processes (from DTA). To further understand each process and the corresponding product of the decomposition or phase transition, three additional independent runs were performed by ramping up to 275 °C, 315 °C, and 355 °C, respectively, slightly above the three thermal processes denoted by (a), (b), and (c). The products from each run were identified by X-ray powder diffraction. The first thermal process (a), with a bulk onset temperature of 239(3) °C, and the first weight loss, correspond to the following equation: $CH_3BiI_2(s) \rightarrow CH_3I(g) + BiI(s)$. The observed weight loss, 29.3%, is in a good agreement with the expected value (29.7%) from the above equation. This is also consistent with the GC/MS study, although the GC/MS study has higher sensitivity and therefore detects the evolution of small amounts of methyl iodide at lower temperatures than the TGA study. The solid product is a mixture of α- and *β*-BiI, primarily *β*-phase, although a trace amount of BiI_3 was also detected from the powder pattern. The mixture of bismuth monoiodides starts to decompose at temperatures above 311(1) °C (process (b) in Figure 12), in good agreement with the expected peritectic decomposition observed for pure BiI at 312 °C by von Schnering et al.[42] The product of this decomposition, solidified from 315 °C, is primarily BiI_3 and a mixture of lower valent bismuth iodides, such as $BiI_{3.3}I$, etc. Transition (c) at 334(2) °C corresponds to the monotectic (expected at around 336°) in the phase diagram of BiI_3−Bi.[43] A small amount of Bi metal, identified from the powder pattern, starts showing up in products of reactions cooled from temperatures above transition (c). The second weight loss from the TGA curve starts at approximately 300 °C and ends at 440 °C and corresponds to the vaporization of BiI_3. Above 440 °C, only bismuth metal was detected in the solid product. The total weight loss up to 440 °C was 74.1%, slightly higher than expected (70.8%), according to the following overall thermal decomposition process: $2CH_3BiI_2 \rightarrow 2CH_3I + {}^2/_3BiI_3 + {}^4/_3Bi$. The extra weight loss may be attributed to the partial loss of intermediates or final products at the higher temperatures of the scan.

Conclusion

The one-step reaction between readily available bismuth metal and methyl iodide under solvothermal conditions yields sizable CH_3BiI_2 crystals. In contrast to classical organometallic compounds, which typically feature isolated molecules or clusters, CH_3BiI_2 belongs to a small class of extended solid state organometallic compounds, having a structure that consists of CH_3BiI_2 chains running along the crystallographic *b*-axis and held together by van der Waals interaction. Bi(III) has a slightly distorted square pyramidal local coordination, with four iodines in the basal plane and one methyl group occupying the apical position. The Bi(III) lone pair is stereochemically active and effectively acts as the sixth ligand, occupying a site trans to each methyl group. An interesting structural feature of this compound is that all the methyl groups are aligned on one side of each BiI_2 chain.

Electronic band structure studies using extended Hückel theory demonstrate that the red needle-like crystals of the title compound are electronically one-dimensional. The highest occupied (valence) band is fairly flat and consists of a Bi lone pair orbital which interacts in an antibonding fashion with the iodine 5p orbitals. The mixing of Bi $6p_x$ into the highest occupied band, which reduces the Bi−C antibonding interaction in this band, provides a natural explanation of the stereochemical activity of the Bi(III) lone pair electrons in this compound. This can be contrasted with BiI_3, for which this mixing does not occur, and Bi(III) adopts an ideal octahedral coordination of six iodines. The lowest unoccupied (conduction) bands are composed primarily of Bi $6p_x$ and $6p_y$ orbitals which are antibonding with respect to the iodine $5p_x$ and $5p_y$ orbitals.

Organobismuth dihalides and related compounds are in general very reactive and decomposed by moisture, alcohols, and ammonia. The organobismuth diiodides appear to be much less reactive than the corresponding bromo or chloro compounds,[33] enabling relatively simple handing in an ambient environment. In addition, we find that in an inert atmosphere, CH_3BiI_2 can be heated to approximately 185 °C without significant decomposition. Above this temperature, thermal decomposition leads to the loss of iodomethane and a new synthetic route to the interesting reduced valent, one-dimensional conducting compound, BiI.

Finally, in analogy with the ionically bonded organic-inorganic layered perovskite compounds, it is expected that other organics may be substituted into this $RBiI_2$ ordered one-dimensional structure. For example, varying alkyl chain length, if possible, might provide some degree of control over the

(42) von Schnering, H. G.; von Benda, H.; Kalveram, C. *Z. Anorg. Allg. Chem.* **1978**, *438*, 37.
(43) Yosim, S. J.; Ransom, L. D.; Sallach, R. A.; Topol, L. E. *J. Phys. Chem.* **1962**, *66*, 28.

electronic interaction between the chains. Substitution of more complex conjugated organics could lead to a larger degree of electronic tunability than observed in intercalated or ionically bonded systems.

Acknowledgment. We thank B. A. Scott and C. Murray for stimulating discussions and J. Zimmerman for GC/MS measurement. H. Genin thanks AT&T Bell Laboratories for a Ph.D. Fellowship.

Supporting Information Available: Table showing anisotropic thermal parameters for CH_3BiI_2 and figure showing projected density-of-states curves, within the one-dimensional CH_3BiI_2 chain model, for bismuth $6p_z$ and $6p_y$ (2 pages). See any current masthead page for ordering and Internet access instructions.

JA961753H